Received: 15 March 2017 | Accepted: 24 May 2017
DOI: 10.1002/jcp.26030

ORIGINAL RESEARCH ARTICLE

WILEY Journal of Cellular Physiology

Integrated transcriptomic and metabolomic analysis reveals adaptive changes of hibernating retinas

Yizhao Luan[1,2] | Jingxing Ou[3] | Vincent P. Kunze[3] | Fengyu Qiao[3] | Yan Wang[1] | Lai Wei[1] | Wei Li[1,3] | Zhi Xie[1]

[1] State Key Laboratory of Ophthalmology, Guangdong Provincial Key Lab of Ophthalmology, Visual Science, Zhongshan Ophthalmic Center, Sun Yat-sen University, Guangzhou, China

[2] School of Life Sciences, Sun Yat-sen University, Guangzhou, China

[3] Retinal Neurobiology Section, National Eye Institute, Bethesda, Maryland

Correspondence
Zhi Xie, StateKey Laboratory of Ophthalmology, Guangdong Provincial Key Lab of Ophthalmology, Visual Science, Zhongshan Ophthalmic Center, Sun Yat-sen University, 54 South Xianlie South Road, Bldg. 3, Guangzhou, China.
Email: xiezhi@gmail.com
Wei Li, Retinal Neurobiology Section, National Eye Institute, 35 Convent Dr, Bldg. 35A, Rm 3F-226, Bethesda, MD 20892.
Email: liwei2@nei.nih.gov

Funding information
Science and Technology Planning Projects of Guangdong Province, Grant number: 2014B030301040; Joint Research Fund for Overseas Natural Science of China, Grant number: 3030901001222; Major Program of Science and Technology of Guangzhou, Grant number: 201607020001; National Natural Science Foundation of China, Grant number: 31471232; National Eye Institute, Grant number: intramural research program; Center for Precision Medicine, SYSU

Hibernation is a seasonally adaptive strategy that allows hibernators to live through extremely cold conditions. Despite the profound reduction of blood flow to the retinas, hibernation causes no lasting retinal injury. Instead, hibernators show an increased tolerance to ischemic insults during the hibernation period. To understand the molecular changes of the retinas in response to hibernation, we applied an integrative transcriptome and metabolome analysis to explore changes in gene expression and metabolites of 13-lined ground squirrel retinas during hibernation. Metabolomic analysis showed a global decrease of ATP synthesis in hibernating retinas. Decreased glucose and galactose, increased beta-oxidation of carnitine and decreased storage of some amino acids in hibernating retinas indicated a shift of fuel use from carbohydrates to lipids and alternative usage of amino acids. Transcriptomic analysis revealed that the down-regulated genes were enriched in DNA-templated transcription and immune-related functions, while the up-regulated genes were enriched in mitochondrial inner membrane and DNA packaging-related functions. We further showed that a subset of genes underwent active alternative splicing events in response to hibernation. Finally, integrative analysis of the transcriptome and metabolome confirmed the shift of fuel use in the hibernating retina by the regulation of catabolism of amino acids and lipids. Through transcriptomic and metabolomic data, our analysis revealed the altered state of mitochondrial oxidative phosphorylation and the shift of energy source in the hibernating retina, advancing our understanding of the molecular mechanisms employed by hibernators. The data will also serve as a useful resource for the ocular and hibernation research communities.

KEYWORDS
13-lined ground squirrel, hibernation, metabolome, retina, RNA-seq

Yizhao Luan and Jingxing Ou contributed equally to this work.

1 | INTRODUCTION

Hibernation is a seasonally adaptive strategy that allows hibernators to live through cold conditions (Melvin & Andrews, 2009) and is viewed as a highly regulated physiological event (Boyer, 1999). During hibernation, small hibernators such as ground squirrels are under a cycle of interbout arousal state and deep torpor state, characterized by nearly freezing body temperature, lower heart rates of 4–6 beats per min and depressed metabolism (Andrews, 2007).

Complex changes in gene expression and metabolic pathways have been found to associate with the drastic physiological fluctuations of hibernators. With the advent of high-throughout techniques, several tissues including liver, brain, skeletal muscle, and adipose tissue from different hibernating animals were analyzed for their genome-wide molecular changes. In general, hibernators showed distinct molecular and cellular changes in the entry, deep torpor, interbout arousal and transitional stages. For example, by applying RNA sequencing to heart, skeletal muscle, and white adipose tissue (WAT) from 13-lined squirrels, it was found that gene expression changes showed highly tissue-specific patterns in response to hibernation (Hampton et al., 2011). Ion transport-related genes were required in the heart for contraction and relaxation in hibernation, while genes in the ubiquitin pathway were enriched in skeletal muscle. In WAT, gene expression switched to low in lipogenesis and high in lipolysis when the season changed from summer to fall and winter. In the heart tissue of 13-lined ground squirrels, integrated transcriptomic and proteomic analysis revealed potential cardio-protective mechanisms associated with splice variants, mutations and genome reorganizations (Vermillion, Jagtap, Johnson, Griffin, & Andrews, 2015). Liquid chromatography–mass spectrometry-based metabolomic analysis on the liver of the ground squirrel revealed significantly seasonal changes in enzyme cofactor metabolism, amino acid catabolism and purine and pyrimidine metabolism (Nelson, Otis, Martin, & Carey, 2009).

The neural retina is a laminated tissue with several layers of different cell types, of which photoreceptors account for a significant portion. Mammalian photoreceptors require a tremendous amount of energy to maintain their normal functions, even compared with other neurons (Kaden & Li, 2013). During hibernation, blood flow is drastically reduced, imposing extreme metabolic challenges on the retinas (Sterling, 1999; Vaughan, Gruber, Michalski, Seidling, & Schlink, 2006). Nonetheless, hibernators did not exhibit accruing permanent cellular damage. In contrast, similar experimental conditions in human and most other mammals often lead to cell death or dysfunction (Dave, Christian, Perez-Pinzon, & Drew, 2012). However, systematic investigation into molecular changes in the retinas during the hibernation season is still lacking. In addition, because the ground squirrel has cone-dominant photoreceptors akin to the human fovea region, this species is well suited to be a model for diseases such as age-related macular degeneration (AMD) and cone dystrophies (Kaden & Li, 2013; Merriman, Sajdak, Li, & Jones, 2016).

In this study, we used RNA sequencing (RNA-seq) and liquid chromatography-mass spectrometry (LC-MS) to profile the changes of transcripts and metabolites in 13-lined ground squirrel (*Ictidomys tridecemlineatus*) retinas in response to hibernation. While ATP synthesis was found to decrease in hibernating retinas, our metabolic analysis illustrated a shift of fuel use from carbohydrates to lipids and alternative usage of amino acids, revealed by the decrease of glucose and galactose, intensive beta-oxidation of lipids and the increase of a urea cycle activator together with the decrease of some amino acids. Transcriptomic analysis identified that DNA-templated transcription and major histocompatibility complex (MHC)-mediated immune responses were down-regulated at the mRNA level, while mitochondrial oxidative phosphorylation and chromatin-DNA reorganization were up-regulated. Differential exon usage analysis indicated that genes underwent active alternative splicing events in response to hibernation. Integrative transcriptomic and metabolomic analysis confirmed the shift of fuel use in the hibernating retina by the regulation of catabolism of amino acids and lipids, and the amino acids used as fuel were probably from protein degradation. Overall, this study deepens our understanding of molecular changes in the retinas of hibernators in response to hibernation and may facilitate the effort in developing therapeutic strategies against metabolic stress often associated with retinal injury and degenerative disease (Cuenca et al., 2014; Inman & Harun-Or-Rashid, 2017; Narayan, Chidlow, Wood, & Casson, 2017).

2 | MATERIALS AND METHODS

2.1 | Animal housing and tissue collection

All animal studies were conducted in accordance with the requirements of the National Eye Institute Animal Review Board, and approved by the Institutional Animal Care and Use Committee at the National Eye Institute, NIH (protocol #NEI-595). Before hibernation season, 13-lined ground squirrels between 5 and 12 months of age were bred with Purina Cat Chow and weekly dry fruit and sun flower seed supplements at 20°C. The lighting in the ground squirrel holding room consists of full spectrum (T8) bulbs, used to mimic the natural daylight spectrum. The photoperiod had been incrementally adjusted every 2 weeks during the squirrel's "awake" period to mimic natural conditions. The Oshkosh, Wisconsin "Sunrise" and "Sunset" times was utilized for the photoperiod adjustments. For active animals in winter season, the housing conditions remained unchanged; for hibernating animals at the same season, they were placed inside individual housing boxes with bedding materials (Tek-Fresh Harlan T.7099) to provide insulation. The boxes were put inside a 4°C hibernaculum with no light. The hibernating animals were inspected weekly in red light to ensure they were in good physiological conditions. All retinal tissues were collected between November and March. On the day of tissue collection, animals were anesthetized quickly by isoflurane inhalation, and sacrificed by decapitation. Hibernating tissues were collected from animals that had entered their hibernation cycle for at least 1 month and had been in the deep torpor phase for at least 3 days. Tissues were collected from both male and female ground squirrels. The winter active animals weighed between 220 and 280 g, and animals from

their hibernating cycle weighed between 140 and 180 g. The collected retinal tissues were then frozen in liquid nitrogen and stored at −80°C.

2.2 | Metabolome analysis

Six animals were used in each group - winter awake (body temperature at −36°C) and deep torpor (body temperature between 2 and 6°C). The extracted tissues were prepared for metabolic profiling following Metabolon's standard solvent extraction method. The samples were split into equal parts for analysis on the GC/MS and LC/MS/MS platforms. A total of 170 metabolites were identified and quantified for awake and hibernating retinas. First, the metabolite intensity for each sample was normalized using the total protein. The total protein concentration was measured by Bradford protein assay. Then, the intensity of each metabolite was rescaled to set the median equal to 1. Lastly, missing values were replaced with the minimum of the normalized values. The metabolites with high missing rates (>0.5) in any condition were removed in subsequent analyses. A Wilcoxon rank-sum test was used to rank metabolic changes based on normalized values. The *p* values from the Wilcoxon rank-sum test were adjusted by false discovery rate (FDR).

2.3 | RNA sequencing experiment and data analysis

For RNA-sequencing analysis, we compared whole-retinal transcriptome changes between winter awake (four animals) and deep torpor (six animals) phase. Total RNAs were extracted from the retinas with TRIzol (Thermo Fisher Scientific, Waltham, MA) and further processed with the TruSeq stranded total RNA sample preparation kit (Illumina, San Diego, CA). RNA-seq was performed using an Illumina HiSeq 2000 sequencer.

Read quality was assessed using the FastQC toolset (v0.10.1) (http://www.bioinformatics.babraham.ac.uk/projects/fastqc). Low-quality bases were removed, and trimmed reads were aligned to the *Ictidomys tridecemlineatus* genome reference (Ensembl spetri2) (Yates et al., 2016) with TopHat v2.0.11 (Trapnell, Pachter, & Salzberg, 2009). The parameter options applied in alignment were "-r 200, -g 20, -p 8, -no-coverage-search, -library-type fr-firststrand." The inner distance between pair ends was estimated by the Picard program (http://picard.sourceforge.net). For quantification of gene expression, only the reads aligned uniquely to exons were counted with the Bioconductor package Rsubread (Liao, Smyth, & Shi, 2013). After the gene counting, DESeq (Anders & Huber, 2010) was used for differential expression analysis. Genes with maximum count per million (CPM) >3 in all the samples were included in further analyses. DEXSeq (Anders, Reyes, & Huber, 2012) was used for differential exon usage analysis. Exons with total counts <20 across all the samples were excluded from further analysis.

We performed principle component analysis (PCA) using scaled gene count per million (CPM) values. The top two PCs were used. Gene ontology (GO) analysis was based on a hypergeometric test using the Bioconductor "piano" package (Väremo, Nielsen, & Nookaew, 2013), with the gene list of interest as foreground and all identified genes as background. GO terms were retrieved from the Ensembl BioMart database (Aken et al., 2016). RPKM (reads per kilobase per million) (Mortazavi, Williams, McCue, Schaeffer, & Wold, 2008) values were used for co-expression analysis between MtR-DEGs and the other DEGs. Pearson's correlation coefficient and adjusted *p* values (0.05 as cutoff) were applied to define the association between correlated genes.

2.4 | Integrative transcriptomic and metabolomic pathway analysis

We used the Bioconductor package iSubpathwayMiner (Li et al., 2013; Li et al., 2009) to integrate the transcriptome and the metabolome. A total of 150 metabolic pathways and 150 non-metabolic pathways from the KEGG database were included (Kanehisa, Sato, Kawashima, Furumichi, & Tanabe, 2016). The changed genes and metabolites were used as foreground. All genes and metabolites present in these pathways were used as background. FDR was applied to correct for multiple comparisons.

2.5 | Real-time quantitative PCR

Retinal total RNAs were prepared from winter awake (two pools of three animals each) and deep torpor (two pools of three animals each) phase (RNAeasy Plus kit; Qiagen, Germantown, MD) and reverse transcribed into cDNA (SuperScript III; First-Strand Synthesis Supermix for qRT-PCR; Thermo Fisher Scientific 11752250) according to the manufacturer's instructions. Real-time quantitative PCR (RT-qPCR) was carried out using Platinum Cybergreen Super Mix with Rox dye (Invitrogen #11733-046, Waltham, MA) on an Applied Biosystems Step one real-time PCR machine. Gene expression changes were quantified using $2^{-\Delta\Delta Ct}$ method, and indicated as means ± SE. The unchanged gene *KCNC1* was used as control gene in the normalization of gene expression in RT-qPCR. Statistical analysis of RT-qPCR was conducted using *t*-test.

3 | RESULTS

3.1 | Metabolite changes and fuel-use shift in hibernating retina

To characterize the metabolic alterations during the deep hibernation stage, we quantified 170 metabolites using mass spectrometry (see section 2 for details). These metabolites fell into eight categories, including amino acids, carbohydrates, co-factors and vitamins, energy, lipids, nucleotides, peptides and xenobiotics (Figure 1a, Supplementary Table S1). To examine the relationship among samples at the metabolic level, we performed PCA, which clearly separated the samples by condition (Figure 1b). The top two PCs explained ~91% of the variance among samples, illustrating the distinguishing metabolic patterns between hibernating retinas and awake ones. A Wilcoxon rank-sum test of metabolite concentration distribution found that the global metabolism in hibernating retinas are significantly lower than those of awake ones ($p = 2.344E-6$, Figure 1c), revealing a global reduction of metabolites in response to deep hibernation.

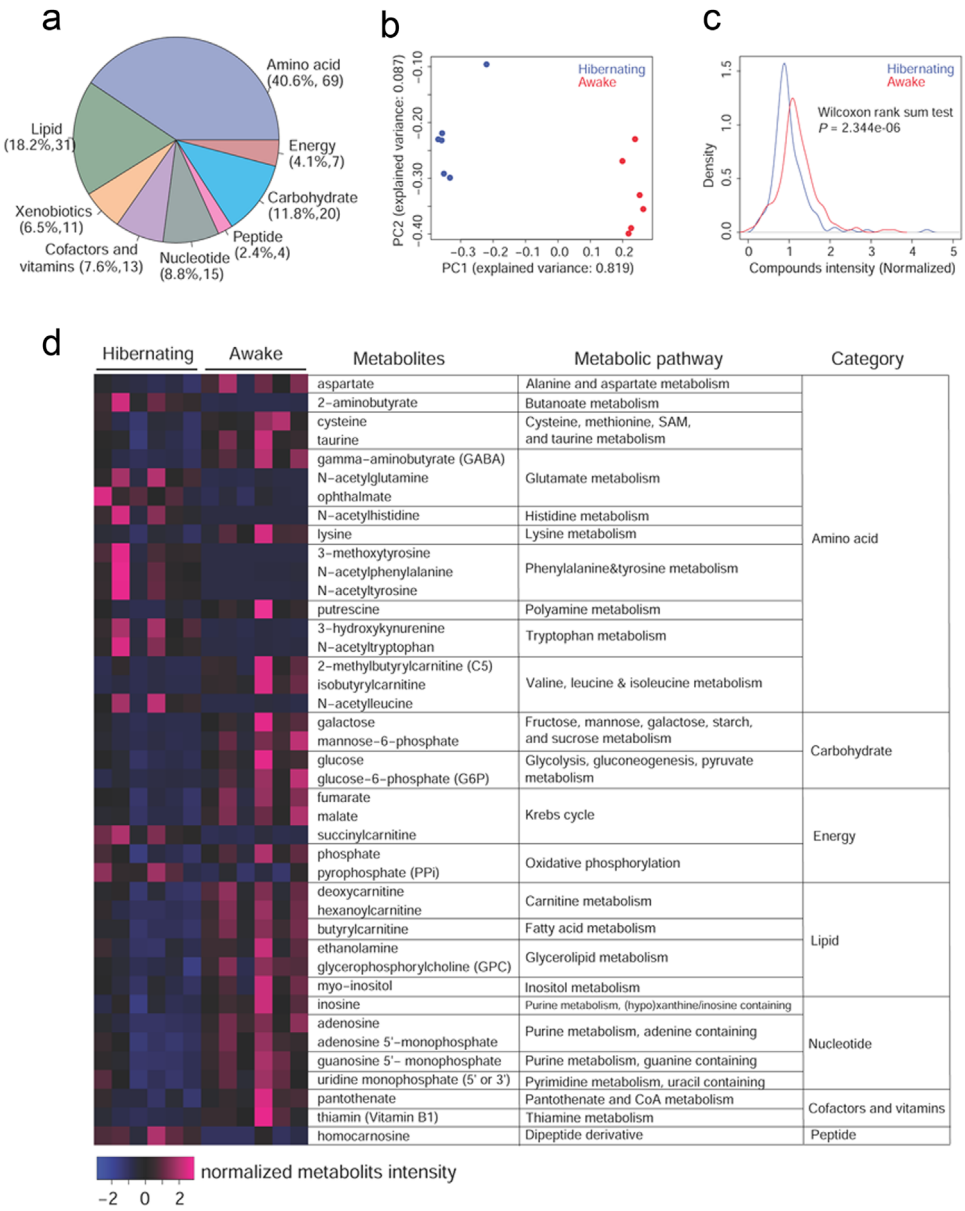

FIGURE 1 Global repression of metabolites in hibernating retina. (a) Metabolite category: 170 metabolites were detected. The category names, ratio and number of metabolites are shown. (b) Principal component analysis (PCA) of normalized metabolite intensity. The top two PCs are plotted. The awake and hibernating groups were clearly separated by the first PC, which explained 81.9% of the variance. (c) Comparison of metabolite levels in the two conditions. Metabolite levels were significantly lower in hibernating retinas than awake ones (Wilcoxon rank-sum test, $p = 2.344 \times 10^{-6}$). (d) Heatmap of intensities of significantly changed metabolites. Differential analysis of metabolite levels in two conditions identified 45 significant metabolites (adjusted $p < 0.1$). The pathway and category annotations of the metabolites are shown

Metabolites are products of biochemical reactions; differences in those components may suggest distinct physiological states. Wilcoxon rank-sum tests found that 45 metabolites were significantly changed with false discovery rate (FDR) < 0.1, including 15 up-regulated and 30 down-regulated metabolites, in hibernating retinas compared to awake ones (Supplementary Table S1). Figure 1d shows all the significant metabolites. Overall, all the down-regulated metabolites in hibernating retinas were associated with to carbohydrate, lipid, nucleotide, cofactor or vitamin metabolism. Specifically, the hibernating retina showed decreases in aspartate (FC = 0.34) and malate (FC = 0.38), which are the main metabolites of malateaspartate shuttle for translocating electrons produced by glycolysis to the mitochondrial electron transport chain. Further, phosphate (FC = 0.61), one of the main materials of ATP synthase, was also found to decrease in the hibernating retina. These findings together revealed a reduction of ATP generation from mitochondrial oxidative phosphorylation. Nevertheless, we found no difference of CoA level between the two conditions (Supplementary Table S1). CoA can be generated by catabolism of carbohydrates, amino acid or lipids. First, we found a reduction of glycolysis and gluconeogenesis, revealed by a decrease of

glucose and galactose in the hibernating retina. Second, multiple acylcarnitine species (deoxy-, butyryl-, isobutyryl-, and hexanoylcarnitine) decreased, indicating intensive beta-oxidation of fatty acids in the hibernating retina. Then, we speculated that amino acid catabolism also increased because of the implication of increased N-acetyl-glutamine (FC = 9.82), an activator of a urea cycle enzyme to remove ammonia, and decreased cysteine, taurine, lysine, and putrescine. At the same time, we found that multiple acetyl amino acids (N-acetyl-glutamine, N-acetyl-histidine, N-acetyl-phenylalanine, N-acetyl-tyrosine, N-acetyl-tryptophan, and N-acetyl-leucine) increased in the hibernating retina. Taken together, these findings imply that hibernating retinas, which generally need less energy than awake ones do, shift their usage of energy sources from mainly carbohydrates to lipids and alternative usage of some amino acids.

3.2 | Expression changes in mRNA and associated functional categories in hibernating retina

To determine the gene expression changes of retinas during hibernation, we performed transcriptome analysis of both hibernating and awake retinas using RNA sequencing. We sequenced six hibernating samples and four awake samples, with ~100 million pair-end reads mapped to the genome per sample, and obtained a total number of 12,647 expressed genes (Supplementary Table S2).

PCA of all the samples separated them into hibernating and awake conditions (Figure 2a). Differentially expressed gene (DEG) analysis further identified 1,591 genes significantly changed in the hibernating condition compared to the awake (adjusted $p < 0.05$), of which 782 genes were up-regulated in hibernation and 809 genes were down-regulated (Supplementary Table S3). Notably, among these DEGs, the top 50 significantly up-regulated genes with fold change >2 included 14 histone protein-coding genes, such as *HIST1H4H* and *H2BFS*. In comparison, the top significantly down-regulated genes with a fold change <0.5 included *COL6A3*, *SPAG6*, *RPE65*, and *TTR*, showing divergent functional involvement.

Compared with gene expression changes in the white adipose tissue (WAT), skeletal muscle, and hearts of 13-lined ground squirrels (Hampton et al., 2011), we found some shared DEGs between different hibernating tissues, even though most of the changed genes were uniquely expressed (Figure 2b). Interestingly, *MYH4* and *PDK4* were shared by all four tissues, but the directions of the gene expression changes were different. While *MYH4* was down-regulated in torpid retinas and skeletal muscle, it was up-regulated in torpid hearts and WAT; *PDK4* was down-regulated in torpid retina but up-regulated during torpor in the other three tissues (Figure 2c). This indicates tissue-specific gene expression changes in hibernating animals.

To explore the biological functions involved in maintaining the hibernating state, we conducted GO analysis (Figure 2d). The GO analysis suggested that the up-regulated DEGs were mainly enriched in nucleosome and chromatin-related terms, such as nucleosome (FDR = 2.18E-21), DNA packaging complex (FDR = 3.68E-20), and chromatin assembly (FDR = 1.17E-12). Unexpectedly, we also found that up-regulated DEGs were enriched in the respiratory-chain-related functional categories, such as the respiratory chain complex (FDR = 8.94E-09) and mitochondrial inner membrane (FDR = 5.00E-6), indicating an active state of oxidative phosphorylation that was opposite to the metabolomic implication of decreased ATP synthesis (Figure 2e; Supplementary Table S4). On the other hand, the down-regulated DEGs were predominantly enriched in transmembrane signaling receptor activity (FDR = 5.13E-5) and MHC-related protein complexes (Figure 2d; Supplementary Table S4), indicating a down-regulation of transmembrane signaling transduction and acquired immunity in the hibernating retina.

3.3 | Transcriptomic up-regulation of oxidative phosphorylation and co-expressed genes

Out of 38 enriched GO terms (adjusted $p < 0.05$) for the up-regulated DEGs in the hibernating retina, 21 terms were related to mitochondrial respiration or oxido-reduction (Supplementary Table S4). The related GO terms to the parent term of 'mitochondrion' (GO: 0005739) are illustrated in Figure 3a; the associated DEGs were defined as mitochondrial respiration-related (MtR) DEGs. A total of 50 MtR-DEGs were obtained, including 41 up-regulated and 9 down-regulated. Particularly, 16 DEGs directly involved in the mitochondrial respiration chain were all significantly up-regulated in the hibernating retina (Supplementary Table S5).

We further applied co-expression analysis to identify non-MtR genes that were significantly correlated with up-regulation of mitochondrial respiration. We identified two groups of non-MtR genes highly correlated with MtR-DEGs ($|R| > 0.8$ and FDR < 0.05), which contained 673–741 genes that were positively and negatively correlated with up-regulated MtR-DEGs, respectively. Interestingly, GO analysis identified that nucleic acid metabolic processes, regulation of primary metabolic processes, metal ion binding, and poly(A) RNA binding were significantly enriched by non-MtR-DEGs negatively correlated with up-regulated MtR-DEGs (Figure 3b). In contrast, the top significant GO categories enriched in the positively correlated non-MtR-DEGs included nucleosome and chromatin assembly (Supplementary Table S6), indicating a co-existence of activated chromatin and DNA complex reorganization and activated oxidative phosphorylation in the hibernating retina.

3.4 | Alternative splicing events showed a functional preference

In the hibernating retinas, we found significant changes in multiple spliceosomal RNAs, including *U2*, *U4*, *U5*, and *U6* (Figure 4a; Supplementary Table S3). This implied that alternative splicing might be involved in the regulation of gene expression in hibernating retinas. Hence, we explored alternative splicing events caused by differential exon usage (DEU).

We found that 792 exons (out of 142,777) from 518 genes (out of 15,240) showed differential usage in hibernators compared to awake

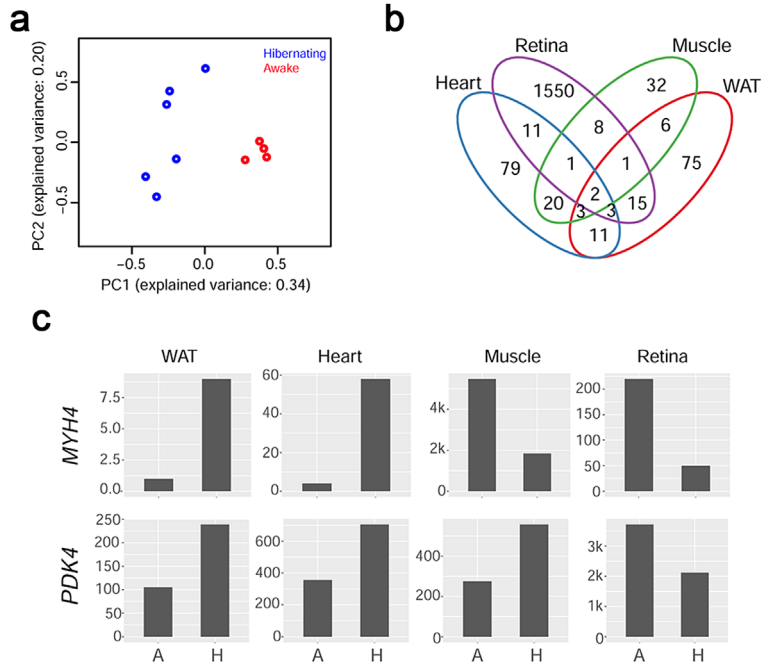

d

Category	GO ID	GO term	Counts	FDR
Up-regulated DEGs				
CC	GO:0000786	nucleosome	32	2.18E-21
CC	GO:0044815	DNA packaging complex	32	3.68E-20
CC	GO:0032993	protein-DNA complex	32	4.09E-16
CC	GO:0070469	respiratory chain	18	2.65E-09
CC	GO:0098803	respiratory chain complex	16	8.94E-09
BP	GO:0006334	nucleosome assembly	32	8.02E-14
BP	GO:0034728	nucleosome organization	33	8.69E-13
BP	GO:0031497	chromatin assembly	32	1.17E-12
BP	GO:0006333	chromatin assembly or disassembly	34	2.06E-12
BP	GO:0065004	protein-DNA complex assembly	32	4.36E-11
MF	GO:0046982	protein heterodimerization activity	35	1.94E-04
MF	GO:0009055	electron carrier activity	12	0.009
MF	GO:0015078	hydrogen ion transmembrane transporter activity	13	0.021
MF	GO:0016675	oxidoreductase activity, acting on a heme group of donors	7	0.021
MF	GO:0016676	oxidoreductase activity, acting on a heme group of donors, oxygen as acceptor	7	0.021
Down-regulated DEGs				
MF	GO:0004888	transmembrane signaling receptor activity	43	5.13E-05
MF	GO:0042605	peptide antigen binding	7	0.021
MF	GO:0003823	antigen binding	9	0.025
CC	GO:0042611	MHC protein complex	9	7.52E-04
CC	GO:0009986	cell surface	31	0.025
CC	GO:0042612	MHC class I protein complex	6	0.025

FIGURE 2 Changes of mRNA expression and associated functional categories (a) PCA of mRNA expression (RPKM) of samples. RPKM values were scaled to (0, 1). The two PCs are shown. The awake and hibernating groups were separated by ~54% explained variance. (b) Numbers of DEGs in hibernating heart, retina, muscle, and white adipose tissue. (c) Expression comparison of *MYH4* and *PDK4* between awake and hibernating tissues. RPKM values are shown. These two genes are shared as DEGs by four tissues. A: awake retina; H: hibernating retina. (d) Gene ontology (GO) analysis for the up- and down-regulated DEGs in the hibernating retina. The top five GO terms with the lowest FDR values within each subcategory (BP, CC, MF) are listed. Counts: the number of DEGs annotated to the GO terms. MF, molecular function. CC, cellular component. BP, biological process

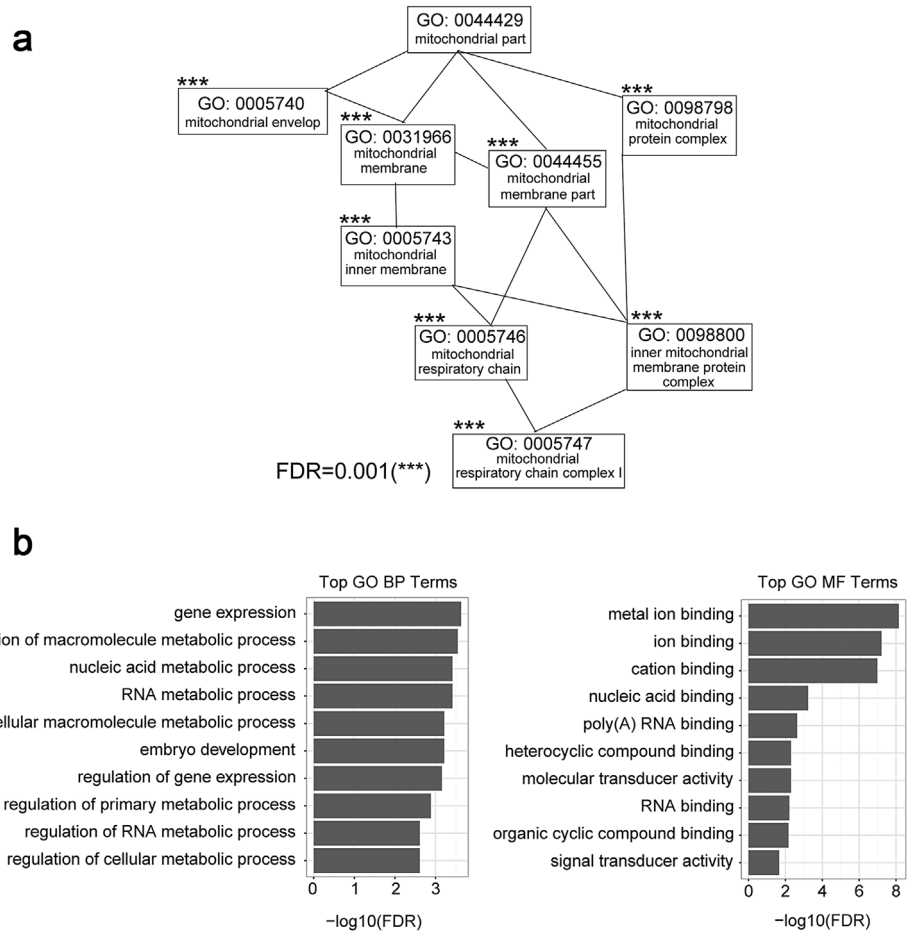

FIGURE 3 Up-regulation of oxidative phosphorylation in hibernating retina (a) Graphical tree model of GO terms relating to "mitochondrion" from GO analysis. Significant terms (adjusted $p \leq 0.05$) are marked with asterisks. *** Indicates adjusted $p < 0.001$. (b) Top enriched GO terms by non-MtR-DEGs negatively correlated with up-regulated MtR-DEGs. BP: biological process; MF: molecular function

animals (adjusted $p < 0.05$; Supplementary Table S7), of which only 71 genes overlapped with the set of DEGs (Figure 4b). 447 genes were not DEGs but contained DEUs, while 1,520 genes were DEGs but did not contain DEUs, indicating differentially used exons and differentially expressed genes complementary to each other to account for the changes in transcriptomic profile in hibernating retinas. For example, *LCA5*, a protein-coding gene of which mutations cause Leber congenital amaurosis (den Hollander et al., 2007), showed significantly differential usages of exons 1, 2, 5, and 7, as exons 1 and 2 were preferred in awake retinas while exon 5 and 7 were preferred in hibernating retinas (Figure 4c). Nevertheless, it was not recognized as a DEG because the total expression levels of the transcripts were about the same. By comparison, *CLK4*, a protein-coding gene regulating alternative splicing of tissue factors (Eisenreich et al., 2009), was identified as a DEG containing DEUs. Figure 4d shows that up-regulation of *CLK4* in the awake condition was caused by up-regulation of all exons, including particularly significant up-regulation of exon 4. The enriched GO terms of genes containing DEUs included RNA binding (adjusted $p = 0.038$), poly(A) RNA binding (adjusted $p = 0.038$), and ubiquitinyl hydrolase activity (adjusted $p = 0.059$) (Figure 4e). The RNA binding cluster can be further divided into four major groups including mRNA processing, translation, RNA splicing, and DNA-templated transcription (Supplementary Table S8). Overall, differential exon usage indicated that genes underwent active alternative splicing events in response to hibernation, revealing a complex landscape of transcriptome changes in retinal cells, together with the DEGs.

3.5 | Confirmation of gene expression by RT-qPCR

We used RT-qPCR to validate the gene expression changes identified in hibernating retina by RNA-seq. A total of 21 significant changed genes in RNA-seq were selected (Supplementary Table S9). These changed genes were mainly involved in biological pathways and molecular functions including metabolism, signaling transduction, acquired immunity and cytoskeleton. The RT-qPCR results confirmed 20 genes with consistent expression changes as shown in RNA-seq experiments, indicating a high reproducibility of transcript abundance assayed by RNA-seq (Figure 5; Supplementary Table S3). These results confirmed the metabolism suppression, down-regulation of signaling transduction and acquired immunity, and cytoskeleton maintenance in hibernating retina.

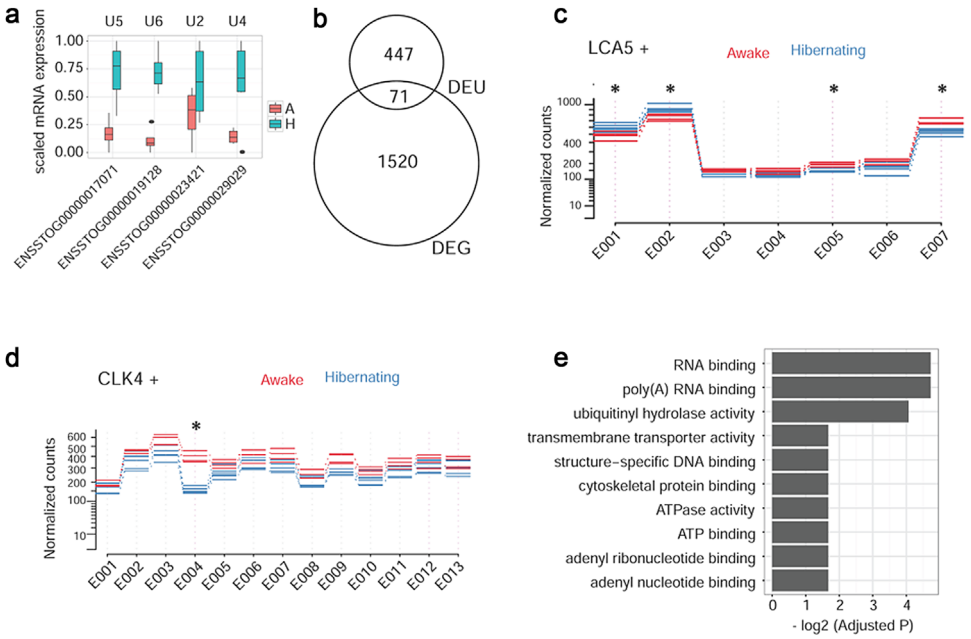

FIGURE 4 Differential exon usage in hibernation retina. (a) Expression comparison of *U2*, *U4*, *U5*, and *U6* identified in RNA-seq. mRNA levels are scaled for unifiedvisualization. Both the Ensembl gene ID and the official gene name are shown. A: awake retina; H: hibernating retina. (b) Comparison of numbers of DEGs and genes with DEUs. (c and d) Visualization of selected genes with differential exon usages. Gene name and strand information are shown on the top. Normalized counts (*Y*-axis) of all exons (*X*-axis) of all samples are shown. Asterisks indicate differentially used exons. (c) *LCA5* was not identified as a DEG, while exons 1, 2, 5, and 7 are used differentially. (d) *CLK4* was identified as both a DEG and a DEU. (e) GO analysis of genes with DEUs. Top GO terms are shown

3.6 | Integrative analysis of mRNAs and metabolite profiling

Given the different states of oxidative phosphorylation revealed by transcriptome and metabolome data, we integrated the data on altered mRNAs and metabolites to reveal the changed biological pathways conclusively. The genes and metabolites were mapped onto 150 metabolic pathways and 150 non-metabolic pathways extracted from iSubpathwayMiner (see section 2). By integrative analysis, we found the involvement of purine metabolism; lysine degradation; glycerolipid metabolism; alanine, aspartate and glutamate metabolism; and pantothenate and CoA biosynthesis in hibernating retinas, confirming the shift of energy source revealed by metabolome analysis (Table 1). Notably, the oxidative phosphorylation pathway was found to be highly enriched for altered metabolic pathways (FDR = 4.55E-9) (Table 1; Supplementary Figure S1), which was consistent with both the transcriptomic changes enriched in mitochondrial respiration and the metabolomic changes in ATP synthesis. This result suggested that oxidative phosphorylation underwent significant and important regulation at both levels.

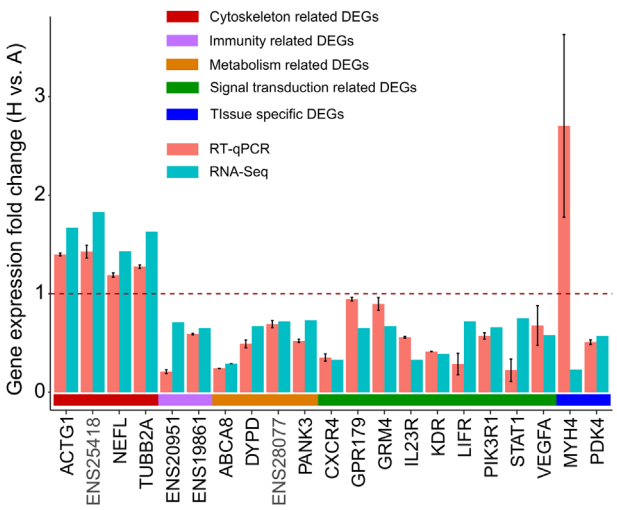

FIGURE 5 Confirmation of gene expression by RT-qPCR. 21 significant genes involved in different functional groups (colored in different colors) are shown. The fold change values of RNA-seq and RT-qPCR are compared

In addition, we identified a number of significantly enriched non-metabolic pathways, including the calcium signaling pathway (FDR = 3.49E-3), the insulin signaling pathway (FDR = 6.99E-3), the MAPK signaling pathway (FDR = 3.73E-2), peroxisomes (FDR = 6.39E-4), and protein digestion and absorption (FDR = 4.95E-4). The changed calcium signaling pathway was consistent with a previous proteomic study, which showed that calcium signaling was significantly reduced during hibernation using the heart tissue of ground squirrels (Vermillion et al., 2015). In addition, down-regulation of insulin signaling and MAPK signaling (Florant & Healy, 2012) and up-regulation of peroxisome functions were also observed previously (Kabine et al., 2003). Protein digestion and absorption suggested the source of the amino acid storage in the hibernating retina. Taken together, the combined analysis of changed mRNAs and metabolites

TABLE 1 Significant KEGG pathways by integration analysis of changed mRNAs and metabolites

Pathway AC	Pathway name	# of hits	Pathway size	Pval	FDR
Path:00190	Oxidative phosphorylation	26	148	4.16E-11	4.55E-09
Path:00230	Purine metabolism	21	253	5.35E-04	6.02E-03
Path:00310	Lysine degradation	10	91	2.01E-03	1.63E-02
Path:00561	Glycerolipid metabolism	9	82	3.34E-03	2.61E-02
Path:00250	Alanine, aspartate, and glutamate metabolism	7	56	4.51E-03	3.31E-02
Path:00770	Pantothenate and CoA biosynthesis	6	43	4.85E-03	3.31E-02
Path:00564	Glycerophospholipid metabolism	11	125	6.92E-03	3.99E-02
Path:04512	ECM-receptor interaction	15	84	4.28E-07	1.87E-05
Path:04510	Focal adhesion	24	201	5.13E-07	1.87E-05
Path:04141	Protein processing in endoplasmic reticulum	20	168	4.66E-06	1.46E-04
Path:04974	Protein digestion and absorption	16	126	1.81E-05	4.95E-04
Path:04146	Peroxisome	12	78	2.92E-05	6.39E-04
Path:03060	Protein export	6	23	1.51E-04	2.75E-03
Path:04020	Calcium signaling pathway	18	187	2.23E-04	3.49E-03
Path:03040	Spliceosome	14	128	2.95E-04	4.04E-03
Path:04540	Gap junction	12	101	3.67E-04	4.72E-03
Path:04260	Cardiac muscle contraction	10	75	4.41E-04	5.37E-03
Path:04122	Sulfur relay system	5	20	6.77E-04	6.99E-03
Path:04910	Insulin signaling pathway	14	140	7.34E-04	6.99E-03
Path:04145	Phagosome	15	161	1.01E-03	8.83E-03
Path:02010	ABC transporters	13	135	1.58E-03	1.33E-02
Path:03320	PPAR signaling pathway	8	72	5.13E-03	3.31E-02
Path:04144	Endocytosis	16	209	5.15E-03	3.31E-02
Path:04142	Lysosome	11	121	5.44E-03	3.40E-02
Path:03010	Ribosome	9	90	6.20E-03	3.73E-02
Path:04010	MAPK signaling pathway	19	271	6.30E-03	3.73E-02

Note: Pathway AC, KEGG pathway ID.
# of hits: the number of DEGs and changed metabolites annotated to the pathway.
Pathway size: the total number of genes and metabolites in the pathway.

not only validated our previous findings but also identified altered genetic pathways in response to hibernation that are not revealed by transcriptomic or metabolomic data sets alone.

4 | DISCUSSION

We profiled the transcriptomic and metabolomic changes of hibernating retinas of 13-lined squirrels during the winter season. Consistent with many previous studies using other hibernating tissues, a global reduction in ATP synthesis was found in hibernating retinas (Barnes, 1989; Tøien et al., 2011). In general, lower metabolic rate, body temperature, and physical activity are considered to be a successful adaptive strategy for hibernators (Melvin & Andrews, 2009). The mode of entry into torpor has been referred to as a regulated suppression of metabolism (Carey, Andrews, & Martin, 2003; Geiser, 2004). A model for the primary source of fuel during hibernation suggests that hibernators may reduce carbohydrate oxidation and rely on the combustion of fat during the hibernating season (Carey et al., 2003; Xu et al., 2013). In our metabolomic analysis, we found decreases of galactose and glucose and intensive beta-oxidation of fatty acids in hibernators, supporting the hypothesized shift of fuel use. As to amino acid catabolism, using amino acids to supply energy in starvation has been thought to put the animal at risk for atrophy (Staples, 2016). Although we found decreases in cysteine, taurine, lysine and putrescine, we also noted the elevation of acetyl amino acids. Given that acetyl modification can make amino acids more stable (Arnesen, 2011), we speculate that the increased storage of acetyl amino acids may be important for hibernators without a steady flow of nutrients from food. It is notable that the increased amino acids in our results were not inconsistent with some previous findings using different tissues and species. For example, the total free amino acid

content of the hibernating optic lobe and diencephalon increased significantly (Watanabe, Shimada, Watanabe, & Nakanishi, 1990), and phenylalanine and tyrosine catabolism were up-regulated during hibernation in two distantly related species of bats (Pan et al., 2013), which may indicate the role of this catabolic pathway in energy supply. In addition, we found an increase in N-acetyltryptophan (Sirianni et al., 2015) that protects protein molecules from oxidative degradation by scavenging oxygen dissolved in protein solutions (Fang, Parti, & Hu, 2011), which may suggest a potential neuroprotective effect. Consistent with previous findings, we observed an increase in 2-aminobutyrate in hibernation, which is a key intermediate in the biosynthesis of ophthalmic acid or ophthalmate, an oxidative stress biomarker (Soga et al., 2006).

RNA synthesis is an energetically expensive process (Carey et al., 2003). It has been revealed that transcription slows down significantly, with UTP incorporation dropping to 11% of euthermic values during torpor compared with aroused hibernators (Bocharova, Gordon, & Arkhipov, 1992). Later, studies on torpid golden-mantled ground squirrels revealed that mRNA synthesis likely ceases within hibernators (van Breukelen & Martin, 2002). Consistent with these findings, we found that down-regulated genes were enriched in gene expression processes, such as the RNA biosynthetic process and DNA-templated transcription. Moreover, we found that genes enriched in the nucleosome and chromatin-related functional categories were significantly up-regulated. Gene expression can be controlled at multiple levels, such as mRNA transcription, processing and stability. Exon usage analysis helps us to understand the involvement of alternative splicing in adaption to the hibernation stage (Stieler et al., 2011). We found that differentially spliced genes have a functional preference toward mRNA processing, translation, RNA splicing and DNA-templated transcription processes. In addition, transcriptomic analysis helped us identify the reduction of multiple metabolic processes including cellular macromolecule metabolic processes, nucleic acid metabolic processes, RNA metabolic processes, and some other regulation processes. These results confirmed our findings from metabolic analysis.

Previous studies on hibernation using liver (Brown, Chung, Belgrave, & Staples, 2012; Brustovetsky, Mayevsky, Grishina, Gogvadze, & Amerkhanov, 1989) as well as skeletal (Brown et al., 2012) and cardiac muscle (Brown & Staples, 2014) have reported that mitochondrial respiration is inhibited in hibernating animals, with different degrees of decline among different tissues or components. Nevertheless, we found that mitochondrial respiration exhibited different states in terms of transcript and metabolite levels within hibernating retinas. While ATP synthesis from mitochondrial respiration decreased during the hibernation season, the genes related to the respiration chain showed active transcriptional up-regulation. The possible reason is that higher expression of these genes within hibernators would allow the rapid production of ATP during arousal from torpor and euthermic interbout arousal, when the demand for energy is high. Taken together, this study may provide novel insights into the molecular mechanisms employed by a hibernator's neuron-enriched tissues.

In light of the ability of hibernating animals to tolerate dramatic fluctuations in blood flow without neurological damage and, experimentally, to survive a variety of neurological insults, it has been hypothesized that some neuroprotective adaptations have been used by hibernators (Drew, Rice, Kuhn, & Smith, 2001; Zhou et al., 2001). It has been proposed that the adaptive strategies may include metabolic suppression, immune inhibition and maintenance of the cytoskeleton (Arendt & Bullmann, 2013; Peretti et al., 2015). In our analysis, both transcriptomic and metabolomic changes provided clues to the neuroprotective strategies adopted by the retina tissue of squirrels. (1) Metabolism suppression. This metabolic suppression was observed in many hibernating animals, such as black bears, golden-mantled ground squirrels, and dormice (Staples, 2014). Consistently, we found that metabolism was repressed globally in the retinas of hibernating 13-lined ground squirrels. A set of metabolic processes, including glycolysis, gluconeogenesis and pyruvate metabolism, RNA metabolic processes, and cellular nitrogen compound metabolic processes, were down-regulated. Although the absence of glucose has been thought to cause photoreceptor death, mitochondrial fuels can enhance cell survival (Chertov et al., 2011). (2) Immune suppression. Hibernation induces suppression of immune responses in mammal species, thus leading to depressed antibody responses and reduced complement activity (Field et al., 2015). Consistent with this view, we found that responses mediated by the major histocompatibility complex (MHC), a set of cell surface proteins essential for the acquired immune system, were suppressed in hibernating retinas (Janeway, Travers, Walport, & Shlomchik, 2011). (3) Cytoskeleton maintenance. The capacity for rapid dendritic regrowth and synaptic rebuilding during hibernation has been observed in the brain (Popov & Bocharova, 1992; Popov, Bocharova, & Bragin, 1992; von der Ohe, Darian-Smith, Garner, & Heller, 2006). Cytoskeletal structural proteins were found to differ between awake and hibernating seasons in the squirrel forebrain by proteomic analysis (Hindle & Martin, 2013). We found enrichment of the term 'structure content of cytoskeleton' (adjusted $p = 0.0093$) by up-regulated genes whose encoded proteins comprise the neuronal cytoskeleton, including *NEFL*, *TUBB2A*, *ACTG1*. Moreover, we found inhibition of ECM-receptor interaction pathways that can repress neuritic outgrowth or cellular interactions. This supports neuroplasticity during hibernation. Taken together, our findings provided supporting evidence for the neuroprotective strategies adopted by hibernators and may shed light on the clinical scenario in which human tissues or cells would be subject to low temperature treatment, such as organ grafting and surgery (Staples, 2016). The drug treatment targeting the identified molecules in our research may also promote survival of the receptor organ. In fact, we have observed elevated cold adaption of human cells after the treatment of drug that can maintain the cytoskeleton structure in another project (data now shown).

In summary, the transcriptomic and metabolomic profiling in this study deepens our understanding of adaptive changes in the retinas of the 13-lined ground squirrel, and it also provides helpful information for further mechanistic investigation concerning, for example, the neuroprotective strategy used by hibernators that can be applied to treatments for retinal injury and degeneration. The

data also serve as a useful resource for the ocular and hibernation research communities.

AUTHORS' CONTRIBUTIONS

Conceived the idea: WL and ZX. Performed data analysis: YZL. Performed laboratory experiments: JXO and LW. RT-PCR: VP and FQ. Wrote the draft: YZL. Interpreted results and improved the manuscript: YZL, JXO, WL, and ZX. All authors edited, read, and approved the final manuscript.

AVAILABILITY OF DATA AND MATERIAL

The sequencing data are deposited at the National Center for Biotechnology Information Gene Expression Omnibus (GEO) database, with accession no. GSE93685, and will be available upon the acceptance of the manuscript.

ACKNOWLEDGMENTS

We thank the members of the Xie and Li laboratories and reviewers for providing valuable suggestions. This work was supported by grants from the National Natural Science Foundation of China (31471232), Science and Technology Planning Projects of Guangdong Province (2014B030301040), Joint Research Fund for Overseas Natural Science of China (3030901001222), Major Program of Science and Technology of Guangzhou (201607020001), and Center for Precision Medicine, SYSU to ZX; this work was also supported by a grant from the National Eye Institute intramural research program to WL.

COMPETING INTERESTS

The author(s) declare that they have no competing interests.

REFERENCES

Aken, B. L., Ayling, S., Barrell, D., Clarke, L., Curwen, V., Fairley, S., . . . Searle, S. M. (2016). The Ensembl gene annotation system. *Database (Oxford)*, *2016*, baw093.

Anders, S., & Huber, W. (2010). Differential expression analysis for sequence count data. *Genome Biology*, *11*(10), R106.

Anders, S., Reyes, A., & Huber, W. (2012). Detecting differential usage of exons from RNA-seq data. *Genome Research*, *22*(10), 2008–2017.

Andrews, M. T. (2007). Advances in molecular biology of hibernation in mammals. *Bioessays*, *29*(5), 431–440.

Arendt, T., & Bullmann, T. (2013). Neuronal plasticity in hibernation and the proposed role of the microtubule-associated protein tau as a "master switch" regulating synaptic gain in neuronal networks. *American Journal of Physiology. Regulatory, Integrative and Comparative Physiology*, *305*(5), R478–R489.

Arnesen, T. (2011). Towards a functional understanding of protein N-terminal acetylation. *PLoS Biology*, *9*(5), e1001074.

Barnes, B. (1989). Freeze avoidance in a mammal: Body temperatures below 0 degree C in an Arctic hibernator. *Science*, *244*(4912), 1593–1595.

Bocharova, L. S., Gordon, R., & Arkhipov, V. I. (1992). Uridine uptake and RNA synthesis in the brain of torpid and awakened ground squirrels. *Comparative Biochemistry and Physiology Part B*, *101*(1–2), 189–192.

Boyer, B. B. (1999). Molecular and metabolic aspects of mammalian hibernation. *Bioscience*, *49*(9), 713–724.

Brown, J. C., Chung, D. J., Belgrave, K. R., & Staples, J. F. (2012). Mitochondrial metabolic suppression and reactive oxygen species production in liver and skeletal muscle of hibernating thirteen-lined ground squirrels. *American Journal of Physiology. Regulatory, Integrative and Comparative Physiology*, *302*(1), R15–R28.

Brown, J. C., & Staples, J. F. (2014). Substrate-specific changes in mitochondrial respiration in skeletal and cardiac muscle of hibernating thirteen-lined ground squirrels. *Journal of Comparative Physiology. B, Biochemical, Systemic, and Environmental Physiology*, *184*(3), 401–414.

Brustovetsky, N. N., Mayevsky, E. I., Grishina, E. V., Gogvadze, V. G., & Amerkhanov, Z. G. (1989). Regulation of the rate of respiration and oxidative phosphorylation in liver mitochondria from hibernating ground squirrels, Citellus undulatus. *Comparative Biochemistry and Physiology. Part B, Biochemistry & Molecular Biology*, *94*(3), 537–541.

Carey, H., Andrews, M. T., & Martin, S. L. (2003). Mammalian hibernation: Cellular and molecular responses to depressed metabolism and low temperature. *Physiological Reviews*, *83*(4), 1153–1181.

Chertov, A. O., Holzhausen, L., Kuok, I. T., Couron, D., Parker, E., Linton, J. D., . . . Hurley, J. B. (2011). Roles of glucose in photoreceptor survival. *Journal Biological Chemistry*, *286*(40), 34700–34711.

Cuenca, N., Fernandez-Sanchez, L., Campello, L., Maneu, V., De la Villa, P., Lax, P., & Pinilla, I. (2014). Cellular responses following retinal injuries and therapeutic approaches for neurodegenerative diseases. *Progress in Retinal and Eye Research*, *43*, 17–75.

Dave, K. R., Christian, S. L., Perez-Pinzon, M. A., & Drew, K. L. (2012). Neuroprotection: Lessons from hibernators. *Comparative Biochemistry and Physiology. Part B, Biochemistry & Molecular Biology*, *162*(1–3), 1–9.

den Hollander, A. I., Koenekoop, R. K., Mohamed, M. D., Arts, H. H., Boldt, K., Towns, K. V., . . . Roepman, R. (2007). Mutations in LCA5, encoding the ciliary protein lebercilin, cause Leber congenital amaurosis. *Nature Genetics*, *39*(7), 889–895.

Drew, K. L., Rice, M. E., Kuhn, T. B., & Smith, M. A. (2001). Neuroprotective adaptations in hibernation: Therapeutic implications for ischemia-reperfusion, traumatic brain injury and neurodegenerative diseases. *Free Radical Biology & Medicine*, *31*(5), 563–573.

Eisenreich, A., Bogdanov, V. Y., Zakrzewicz, A., Pries, A., Antoniak, S., Poller, W., . . . Rauch, U. (2009). Cdc2-like kinases and DNA topoisomerase I regulate alternative splicing of tissue factor in human endothelial cells. *Circulation Research*, *104*(5), 589–599.

Fang, L., Parti, R., & Hu, P. (2011). Characterization of N-acetyltryptophan degradation products in concentrated human serum albumin solutions and development of an automated high performance liquid chromatography-mass spectrometry method for their quantitation. *Journal of Chromatography. A*, *1218*(41), 7316–7324.

Field, K. A., Johnson, J. S., Lilley, T. M., Reeder, S. M., Rogers, E. J., Behr, M. J., & Reeder, D. M. (2015). The white-nose syndrome transcriptome: Activation of anti-fungal host responses in wing tissue of hibernating little brown myotis. *PLoS Pathogens*, *11*(10), e1005168.

Florant, G. L., & Healy, J. E. (2012). The regulation of food intake in mammalian hibernators: A review. *Journal of Comparative Physiology B Biochemical Systemic and Environmental Physiology*, *182*(4), 451–467.

Geiser, F. (2004). Metabolic rate and body temperature reduction during hibernation and daily torpor. *Annual Review of Physiology*, *66*, 239–274.

Hampton, M., Melvin, R. G., Kendall, A. H., Kirkpatrick, B. R., Peterson, N., & Andrews, M. T. (2011). Deep sequencing the transcriptome reveals seasonal adaptive mechanisms in a hibernating mammal. *PLoS ONE*, *6*(10), e 27021.

Hindle, A. G., & Martin, S. L. (2013). Cytoskeletal regulation dominates temperature-sensitive proteomic changes of hibernation in forebrain of 13-lined ground squirrels. *PLoS ONE*, *8*(8), e71627.

Inman, D. M., & Harun-Or-Rashid, M. (2017). Metabolic vulnerability in the neurodegenerative disease glaucoma. *Front Neuroscience*, *11*, 146.

Janeway, C. A. Jr, Travers, P., Walport, M., & Shlomchik, M. J. (2001). *Immunobiology*. New York: Garland Science.

Kabine, M., Clemencet, M. C., Bride, J., El Kebbaj, M. S., Latruffe, N., & Cherkaoui-Malki, M. (2003). Changes of peroxisomal fatty acid metabolism during cold acclimatization in hibernating jerboa (*Jaculus orientalis*). *Biochimie*, *85*(7), 707–714.

Kaden, T. R., & Li, W. (2013). Autophagy, mitochondrial dynamics and retinal diseases. *Asia-Pacific Journal of Ophthalmology (Philadelphia)*, *2*(5), 341–348.

Kanehisa, M., Sato, Y., Kawashima, M., Furumichi, M., & Tanabe, M. (2016). KEGG as a reference resource for gene and protein annotation. *Nucleic Acids Research*, *44*(D1), D457–D462.

Li, C., Han, J., Yao, Q., Zou, C., Xu, Y., Zhang, C., … Li, X. (2013). Subpathway-GM: Identification of metabolic subpathways via joint power of interesting genes and metabolites and their topologies within pathways. *Nucleic Acids Research*, *41*(9), e101.

Li, C., Li, X., Miao, Y., Wang, Q., Jiang, W., Xu, C., … Xu, L. (2009). SubpathwayMiner: A software package for flexible identification of pathways. *Nucleic Acids Research*, *37*(19), e131.

Liao, Y., Smyth, G. K., & Shi, W. (2013). The Subread aligner: Fast, accurate and scalable read mapping by seed-and-vote. *Nucleic Acids Research*, *41*(10), e108.

Melvin, R. G., & Andrews, M. T. (2009). Torpor induction in mammals: Recent discoveries fueling new ideas. *Trends in Endocrinology and Metabolism*, *20*(10), 490–498.

Merriman, D. K., Sajdak, B. S., Li, W., & Jones, B. W. (2016). Seasonal and post-trauma remodeling in cone-dominant ground squirrel retina. *Experimental Eye Research*, *150*, 90–105.

Mortazavi, A., Williams, B. A., McCue, K., Schaeffer, L., & Wold, B. (2008). Mapping and quantifying mammalian transcriptomes by RNA-Seq. *Nature Methods*, *5*(7), 621–628.

Narayan, D. S., Chidlow, G., Wood, J. P., & Casson, R. J. (2017). Glucose metabolism in mammalian photoreceptor inner and outer segments. *Journal of Clinical & Experimental Ophthalmology*, https://doi.org/10.1111/ceo.12952

Nelson, C. J., Otis, J. P., Martin, S. L., & Carey, H. V. (2009). Analysis of the hibernation cycle using LC-MS-based metabolomics in ground squirrel liver. *Physiological Genomics*, *37*(1), 43–51.

Pan, Y. H., Zhang, Y., Cui, J., Liu, Y., McAllan, B. M., Liao, C. C., & Zhang, S. (2013). Adaptation of phenylalanine and tyrosine catabolic pathway to hibernation in bats. *PLoS ONE*, *8*(4), e62039.

Peretti, D., Bastide, A., Radford, H., Verity, N., Molloy, C., Martin, M. G., … Mallucci, G. R. (2015). RB M3 mediates structural plasticity and protective effects of cooling in neurodegeneration. *Nature*, *518*(7538), 236–239.

Popov, V. I., & Bocharova, L. S. (1992). Hibernation-induced structural changes in synaptic contacts between mossy fibres and hippocampal pyramidal neurons. *Neuroscience*, *48*(1), 53–62.

Popov, V. I., Bocharova, L. S., & Bragin, A. G. (1992). Repeated changes of dendritic morphology in the hippocampus of ground squirrels in the course of hibernation. *Neuroscience*, *48*(1), 45–51.

Sirianni, A. C., Jiang, J., Zeng, J., Mao, L. L., Zhou, S., Sugarbaker, P., … Wang, X. (2015). N-acetyl-l-tryptophan, but not N-acetyl-d-tryptophan, rescues neuronal cell death in models of amyotrophic lateral sclerosis. *Journal of Neurochemistry*, *134*(5), 956–968.

Soga, T., Baran, R., Suematsu, M., Ueno, Y., Ikeda, S., Sakurakawa, T., … Tomita, M. (2006). Differential metabolomics reveals ophthalmic acid as an oxidative stress biomarker indicating hepatic glutathione consumption. *Journal of Biological Chemistry*, *281*(24), 16768–16776.

Staples, J. F. (2014). Metabolic suppression in mammalian hibernation: The role of mitochondria. *Journal of Experimental Biology*, *217*(Pt 12), 2032–2036.

Staples, J. F. (2016). Metabolic flexibility: Hibernation, torpor, and estivation. *Comprehensive Physiology*, *6*(2), 737–771.

Sterling, P. (1999). Deciphering the retina's wiring diagram. *Nature Neuroscience*, *2*(10), 851–853.

Stieler, J. T., Bullmann, T., Kohl, F., Tøien, Ø., Brückner, M. K., Härtig, W., … Arendt, T. (2011). The physiological link between metabolic rate depression and tau phosphorylation in mammalian hibernation. *PLoS ONE*, *6*(1), e14530.

Tøien, Ø, Blake, J., Edgar, D. M., Grahn, D. A., Heller, H. C., & Barnes, B. M. (2011). Hibernation in black bears: Independence of metabolic suppression from body temperature. *Science*, *331*(6019), 906–909.

Trapnell, C., Pachter, L., & Salzberg, S. L. (2009). TopHat: Discovering splice junctions with RNA-Seq. *Bioinformatics*, *25*(9), 1105–1111.

van Breukelen, F., & Martin, S. L. (2002). Reversible depression of transcription during hibernation. *Journal of Comparative Physiology B*, *172*(5), 355–361.

Väremo, L., Nielsen, J., & Nookaew, I. (2013). Enriching the gene set analysis of genome-wide data by incorporating directionality of gene expression and combining statistical hypotheses and methods. *Nucleic Acids Research*, *41*(8), 4378–4391.

Vaughan, D. K., Gruber, A. R., Michalski, M. L., Seidling, J., & Schlink, S. (2006). Capture, care, and captive breeding of 13-lined ground squirrels, Spermophilus tridecemlineatus. *Lab Animal (NY)*, *35*(4), 33–40.

Vermillion, K. L., Jagtap, P., Johnson, J. E., Griffin, T. J., & Andrews, M. T. (2015). Characterizing cardiac molecular mechanisms of mammalian hibernation via quantitative proteogenomics. *Journal of Proteome Research*, *14*(11), 4792–4804.

von der Ohe, C. G., Darian-Smith, C., Garner, C. C., & Heller, H. C. (2006). Ubiquitous and temperature-dependent neural plasticity in hibernators. *Journal of Neuroscience*, *26*(41), 10590–10598.

Watanabe, M., Shimada, M., Watanabe, H., & Nakanishi, M. (1990). Amino acid content in several brain regions of the active and hibernating frog, Rana esculenta. *Comparative Biochemistry and Physiology. Part B*, *97*(3), 605–610.

Xu, Y., Shao, C., Fedorov, V. B., Goropashnaya, A. V., Barnes, B. M., & Yan, J. (2013). Molecular signatures of mammalian hibernation: Comparisons with alternative phenotypes. *BMC Genomics*, *14*, 567.

Yates, A., Akanni, W., Amode, M. R., Barrell, D., Billis, K., Carvalho-Silva, D., … Flicek, P. (2016). Ensembl 2016. *Nucleic Acids Research*, *44*(D1), D710–D716.

Zhou, F., Zhu, X., Castellani, R. J., Stimmelmayr, R., Perry, G., Smith, M. A., & Drew, K. L. (2001). Hibernation, a model of neuroprotection. *American Journal Pathology*, *158*(6), 2145–2151.

SUPPORTING INFORMATION

Additional Supporting Information may be found online in the supporting information tab for this article.

How to cite this article: Luan Y, Ou J, Kunze VP, et al. Integrated transcriptomic and metabolomic analysis reveals adaptive changes of hibernating retinas. *J Cell Physiol*. 2017;1–12. https://doi.org/10.1002/jcp.26030